

Covalently Attached Liquids: Instant Omniphobic Surfaces with Unprecedented Repellency

Liming Wang and Thomas J. McCarthy*

Abstract: Recent strategies to prepare “omniphobic” surfaces have demonstrated that minimizing contact angle hysteresis (CAH) is the key criterion for effectiveness. CAH is affected by chemistry and topography defects at the molecular and higher levels, thus most surfaces exhibit significant CAH. Preparative methods for stable coatings on smooth substrates with negligible CAH ($< 2^\circ$) for a broad range of liquids have not been reported. In this work, we describe a simple and rapid procedure to prepare omniphobic surfaces that are stable under pressure and durable at elevated temperatures. Consistent with theory, they exhibit sliding angles that decrease with liquid surface tension. Slippery omniphobic covalently attached liquid (SOCAL) surfaces are obtained through acid-catalyzed graft polycondensation of dimethyldimethoxysilane. The smooth, stable, and temperature-resistant coatings show extremely low CAH ($\leq 1^\circ$) and low sliding angles for liquids that span surface tensions from 78.2 to 18.4 mN m⁻¹.

The wetting of solids by liquids is controlled by natural surfaces as well as in innumerable technologies that confront or require a liquid–solid interface. Lotus leaves, butterfly wings, raincoats, and microfluidic devices are examples from an infinite list.^[1] Liquid repellency has been the focus of both practical application and fundamental research for decades.^[2] The development of fluoropolymers^[3] and methylsilicones^[4] in the 1940s emphasized that synthetic materials can be superior to natural ones, and the 2000s realization^[5] that biological topographies can be mimicked to accentuate chemical effects continues to drive studies in “superhydrophobicity”. Contact angle (CA) analysis has been a central method to characterize and compare surfaces. A drop of a particular liquid can form many different static (metastable) contact angles with a given surface, but unique maximum and minimum angles—the dynamic advancing and receding angles (θ_A , θ_R)—can be measured. The events that occur at the contact line are critical to repellency. A drop must distort from a section of a sphere in order to move if there is a difference between θ_A and θ_R , and this difference ($\Delta\theta = \theta_A - \theta_R$) is termed CA hysteresis (CAH). Distorting the drop requires applying a force, and this is usually quantified by measuring the sliding angle. Equation (1) relates the force and CAH:

$$mg(\sin \alpha)/w = \gamma_{LV}(\cos \theta_R - \cos \theta_A) \quad (1)$$

where m and w are the mass and width of the drop, g is the gravitational acceleration, α is the sliding angle, and γ_{LV} is the liquid surface tension.^[6] We emphasize that the sliding angle should decrease with both decreasing liquid surface tension and decreasing CAH. Sliding angles are often reported, but literature values are difficult to correlate or compare. They depend on drop volume, width, and the initial static CA, values of which are generally not reported.

The simultaneous incorporation of topographic features and low surface energy chemistry has been the typical strategy to enhance surface repellency (mostly to water).^[2c,7] If a liquid does not penetrate the features, the contact line becomes discontinuous, and both the advancing and receding CAs increase, the activation barriers for advancing and receding events decrease, and CAH decreases.^[8] This strategy requires that the topographic features support metastable contact lines and prevent the penetration of liquid into the space between them. An inherent problem with this approach is that at sufficient pressure (Laplace pressure), intrusion will occur, and repellency will fail, thus the liquid will intrude at a critical submersion depth, and drops of the liquid that impinge on these surfaces above a certain velocity will not be repelled. This pressure depends on the geometry of the features, the surface chemistry, and the liquid surface tension. Thus many surfaces are “superhydrophobic” (water $\gamma_{LV} \approx 72$ mN m⁻¹), but few are “superomniphobic” (most organic liquids have $\gamma_{LV} < 30$ mN m⁻¹).^[9] Additional problems with this strategy are that topographic features are usually fragile, surfaces can be fouled by contaminants, and condensation can induce intrusion. A second strategy for omniphobicity involves smooth, liquid-infused porous surfaces (SLIPs) that are “liquid-like”. SLIPs do not require pressure-dependent metastable states, but involve dynamic liquid/liquid/vapor contact line motion.^[10] This approach has led to exceptional properties, including self-healing and anti-icing, but has the obvious complexity of requiring a mobile liquid that can be depleted and must be both immiscible with and not displaceable by the contacting liquid medium. A third strategy is to introduce covalently attached flexible groups onto smooth surfaces.^[11] The grafted groups impart a liquid-like quality to solid objects and are not dissolved or displaced by contacting liquids. This approach suffers from the complexity and duration of preparative methods.

Herein, we report a simple and straightforward method to prepare omniphobic surfaces that we believe to be as good or better than reported methods. In particular, sliding angles that are consistent with theoretical predictions were observed for the first time. Complex synthetic-chemistry techniques or

[*] Dr. L. Wang, Prof. Dr. T. J. McCarthy
Polymer Science and Engineering Department
University of Massachusetts
120 Governors Drive, Amherst MA (USA)
E-mail: tmcc@umass.edu

Supporting information for this article is available on the WWW under <http://dx.doi.org/10.1002/anie.201509385>.

long reaction times were not required, and slippery omniphobic covalently attached liquid (SOCAL) surfaces were obtained through acid-catalyzed graft polycondensation of dimethyldimethoxysilane.

The procedure (Figure 1a) can be termed “instant” as it takes only minutes at room temperature or seconds at elevated temperature. It entails dip-coating a substrate in an isopropanol solution of $\text{Me}_2\text{Si}(\text{OMe})_2$ and sulfuric acid,

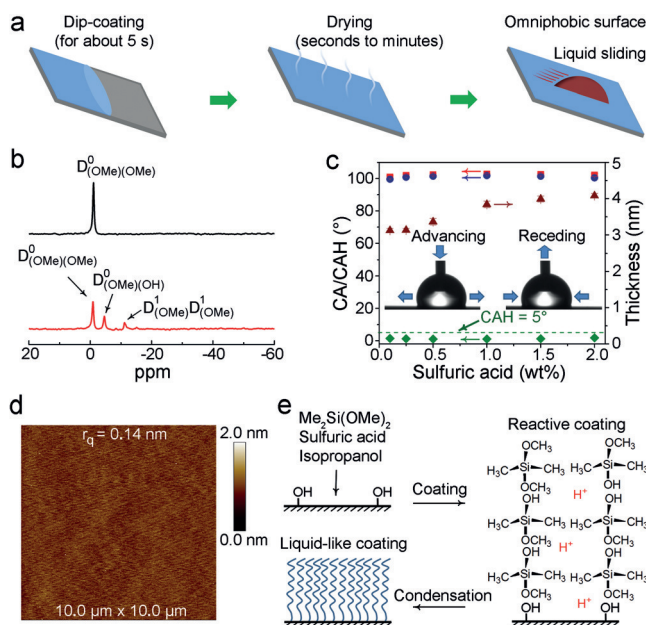


Figure 1. a) Preparation of the omniphobic $\text{Me}_2\text{Si}(\text{OMe})_2$ derived SOCAL PDMS coating. b) ^{29}Si NMR spectra of dimethyldimethoxysilane (10 wt%) in pure isopropanol (top) and in isopropanol containing 1.0 wt% of sulfuric acid (bottom) 12 h after preparation. D^0 represents monomeric D species, whereas D^1 represents a dimer of D species. c) Variation of the water θ_A (■), θ_R (●), and CAH ($\Delta\theta$, ◆) on the $\text{Me}_2\text{Si}(\text{OMe})_2$ derived substrates and the corresponding ellipsometric thickness values (▲) of the coatings as a function of sulfuric acid concentration (wt%). The substrates were dried for 15 min at 21 °C. d) Topographic image of the SOCAL coating on a silicon wafer. e) Formation of the SOCAL PDMS coating by rapid acid-catalyzed polycondensation of dimethyldimethoxysilane on a substrate surface.

drying at room temperature, and rinsing the substrate with water, isopropanol, and toluene. Omniphobicity is apparent during rinsing. H_2SO_4 is a versatile catalyst for siloxane equilibration, and we studied different polydimethylsiloxane (PDMS) samples, organosilicon compounds, various solvents, and multiple reaction conditions (see the Supporting Information, Tables S1, S2 and Figure S1). $\text{Me}_2\text{Si}(\text{OMe})_2$ and isopropanol were identified as the most promising system. Analysis of the $\text{Me}_2\text{Si}(\text{OMe})_2$ /sulfuric acid/isopropanol solution by ^{29}Si NMR spectroscopy indicates that polymerization does not occur in solution. Figure 1b shows spectra of a solution twelve hours after preparation. PDMS oligomers or polymers would exhibit a resonance at $\delta \approx -22$ ppm in isopropanol (Figure S2), which was not observed. We assigned the peaks at $\delta = -4.5$ and -11.1 ppm to $\text{Me}_2\text{Si}(\text{OH})\text{OMe}$ and $(\text{MeO})\text{Me}_2\text{Si}-\text{O}-\text{SiMe}_2(\text{OMe})$, respec-

tively.^[12] Polymerization of $\text{Me}_2\text{Si}(\text{OMe})_2$ occurred upon its concentration during the drying step in air and not while the substrate was in contact with the bulk solution. We note that water is a co-monomer in this polymerization and that drying in low-humidity environments can lead to surfaces with higher CAH (Table S3). Water CA data for surfaces prepared with different sulfuric acid concentrations is presented in Figure 1c. All of these surfaces exhibited high water CAs (θ_A , $\theta_R \geq 100^\circ$) and low CAH ($\Delta\theta < 2^\circ$), and the sample prepared with 1.0 wt% H_2SO_4 exhibited $\Delta\theta = 1^\circ$. Images of these measurements are included in Figure 1c, showing the advancing and receding events for a 4 μL water drop on a SOCAL surface ($\theta_A/\theta_R = 102.8^\circ/101.8^\circ$). Figure 1c shows that a 3–4 nm thick coating was formed; we attribute the small increase in thickness with increasing H_2SO_4 concentration to the water that is present in the H_2SO_4 . Figure 1d shows an atomic force microscope (AFM) topographic image of a SOCAL coating with a water CAH of $\Delta\theta = 1^\circ$. The coating is extremely smooth, exhibiting sub-nanometer scale roughness ($r_q \approx 0.14$ nm). The homogeneity of the coating is important for minimizing surface CAH (Figure S3). The overall process is summarized in Figure 1e. Coating a substrate with the low-surface-tension $\text{Me}_2\text{Si}(\text{OMe})_2$ /sulfuric acid/isopropanol solution forms a reactive thin liquid film; during the drying step, sulfuric acid catalyzes the hydrolysis and condensation of $\text{Me}_2\text{Si}(\text{OMe})_2$, which leads to the rapid grafting of PDMS to the surface and the formation of a SOCAL coating. Rinsing removes non-covalently attached silicone products and residual sulfuric acid.

We studied the drying step in detail both at room temperature (21 °C) and in an oven (75 °C). CA and ellipsometry data for samples that were allowed to dry for various durations at room temperature are given in Figure 2a,b. The thickness of the grafted PDMS layer increases rapidly over the first 10 min, then this increase levels off. Samples prepared with a drying time of 20 min exhibited thicknesses of 4.0 ± 0.1 nm and a water CAH of $\Delta\theta = 1^\circ$. Samples that were dried for 60 min exhibited thicknesses of 4.7 ± 0.1 nm and greater hysteresis ($\Delta\theta = 3^\circ$). Longer drying times (Figure 2b) yielded surfaces that exhibited much greater CAH and thickness, indicating that coating degradation occurred at longer drying (reaction) times. Drying the samples in an oven at 75 °C significantly increased the rate of PDMS formation. Samples dried for 15 and 20 s exhibited thicknesses of 2.2 ± 0.1 nm and 2.6 ± 0.2 nm, but also slightly greater CAH ($\Delta\theta = 4.8^\circ$ after 15 s and $\Delta\theta = 3.6^\circ$ after 20 s; Figure 2c), indicating that these surfaces are less homogeneous than those prepared at room temperature. Longer drying times eventually led to completely degraded surfaces (Figure 2d). We emphasize that this procedure takes less than 20 s at elevated temperature rather than 20 min at room temperature but the hysteresis is slightly greater.

These results are consistent with step growth polymerization of hydrolyzed $\text{Me}_2\text{Si}(\text{OMe})_2$ catalyzed by sulfuric acid. The gradual build-up in molecular weight, apparent from the ellipsometry data (Figure 2a,c), demonstrates that covalently attached chains are formed by a “grafting from” mechanism. As the concentration of PDMS increases and the monomer concentration decreases, acid-catalyzed equilibration of the

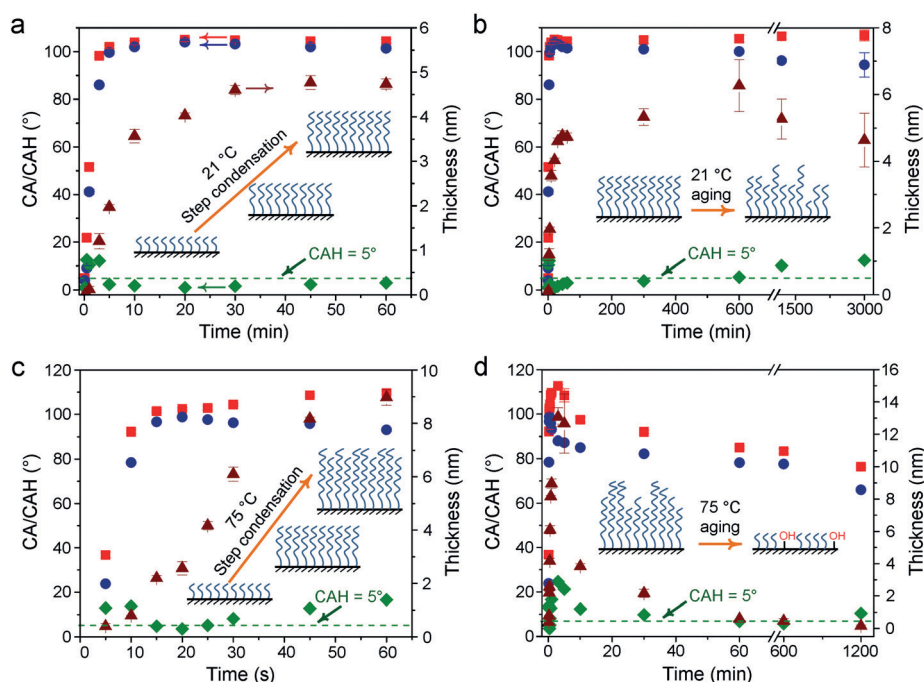


Figure 2. Kinetics of the surface reaction: a–d) Variation of the water θ_A (■), θ_R (●), and CAH ($\Delta\theta$, ◆) on the $\text{Me}_2\text{Si}(\text{OMe})_2$ derived coatings and the corresponding ellipsometric thickness values (\blacktriangle) of the coating as a function of drying time at 21 °C (a,b) and 75 °C (c,d). A greater error in thickness indicates a less uniform PDMS coating. The insets illustrate PDMS growth on substrates based on thickness and standard deviation data.

siloxane chains to volatile cyclic oligomers becomes more important and leads to the observed degradation (Figures S2 and S4). This chemistry has significant precedence.^[13]

We emphasize that the SOCAL coating with minimum water CAH (20 min, 21 °C) also shows excellent oleophobicity, which is demonstrated in Figure 3a–c, which shows the behavior of 20 μL toluene sessile drops (containing Oil Red O) on tilted surfaces. On a clean glass slide (Figure 3a), the toluene drop ($\theta_A/\theta_R = 0^\circ/0^\circ$) spreads on the slide, leaving a large wetting footprint. On a surface containing a monolayer of perfluoroalkyl groups ($\theta_A/\theta_R = 65.6^\circ/50.2^\circ$), a small wetting area is observed, but the drop does not slide owing to the high toluene CAH ($\Delta\theta = 15.4^\circ$; Figure 3b). When a drop is applied to the $\text{Me}_2\text{Si}(\text{OMe})_2$ derived SOCAL surface, it slides immediately, leaving no visible wetting footprint, even though the CA values are low ($\theta_A/\theta_R = 32.0^\circ/31.8^\circ$; Figure 3c and Movie S1). The grafted PDMS coating functions as a liquid phase that is approximately 150 °C above its glass transition temperature. The chain motions are sufficient to almost eliminate barriers to advancing and receding events, resulting in low toluene CAH ($\Delta\theta = 0.2^\circ$).

With regard to the CA data as well as the sliding angle data for the SOCAL coating shown in Table 1, several points are important: 1) The CA values indicate very low hysteresis ($\Delta\theta \leq 1^\circ$) for all liquids, showing broad omniphobicity. These are the lowest CAH values ever reported for flat repellent surfaces. 2) The sliding angle decreases with decreasing liquid surface tension; this is both predicted from Eq. (1) and would be expected of a surface deemed omniphobic. We point out

that this SOCAL surface is the first to demonstrate this trend and the first verification of this prediction. In contrast, sliding angles are not surface-tension-dependent on SLIPS surfaces (Figure S5b).^[10a] This independence suggests the “cloaking” of the probe fluid drop with the SLIPS liquid. Sliding angles increase with decreasing liquid surface tension on topography-based omniphobic surfaces (Figure S5c,d).^[9a,c,14] This indicates increasing contact line pinning (greater intrusion) with decreasing liquid surface tension. 3) Eq. (1) was used to calculate the sliding angles, α^* (Figure S6). The observed sliding angles (Table 1) are higher than those calculated using the equation, but in the same sequence as the predicted ones. 4) A 5 μL hexane sessile drop, which has a lower surface tension than PDMS (liquid $\gamma_{\text{LV}} = 19.0 \text{ mN m}^{-1}$ at 20 °C), slides down a SOCAL surface tilted by 1°. The sliding gradually slows down owing to fast evaporative mass loss from the low contact angle, high surface-area to volume ratio hexane drop (Figure 3d and Movie S2).

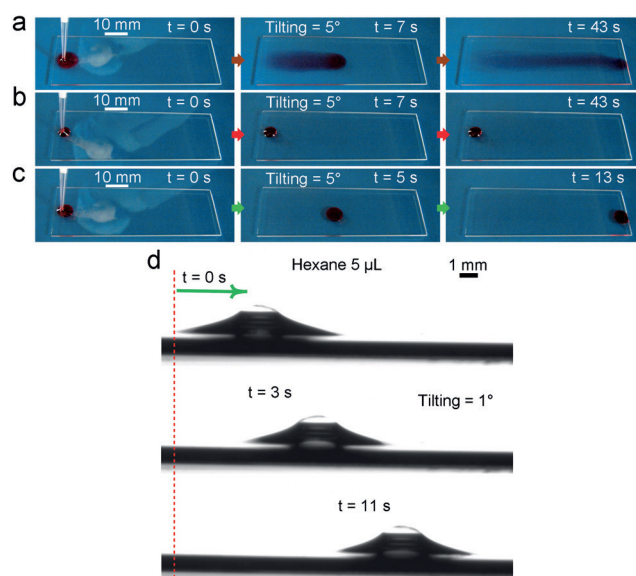


Figure 3. a–c) Time-sequence images for comparison of the mobility of 20 μL toluene drops (containing Oil Red O) on a clean glass slide surface (a), on a clean glass slide modified with $\text{CF}_3-(\text{CF}_2)_5\text{CH}_2\text{CH}_2\text{SiMe}_2\text{Cl}$ (b), and on a clean glass slide coated with a SOCAL PDMS layer (c). d) Time-sequence images for a hexane drop sliding down a tilted SOCAL PDMS surface; a small air bubble was injected on the top of the droplet to increase visibility.

Table 1: Comparison of the CAs (θ_A/θ_R), CAHs ($\Delta\theta$), and the calculated and observed sliding angles (α^* and α) of liquid drops with different volumes (3/20 μL) on the SOCAL PDMS coating.

| Liquid | Surface tension ^[a] [mN m ⁻¹] | CA (θ_A/θ_R) [°] | CAH ($\Delta\theta$) [°] | α^* (3/20 μL) [°] | α (3/20 μL) [°] |
|---------------|---|-----------------------------------|-------------------------------|---|---------------------------------------|
| water | 72.8 | 104.6/103.6 | 1.0 | 4.7/1.3 | 8/4 |
| diiodomethane | 50.8 | 71.2/70.2 | 1.0 | 1.3/0.4 | 4/2 |
| toluene | 28.4 | 32.0/31.8 | 0.2 | 0.4/0.1 | 2/1 |
| hexadecane | 27.5 | 38.6/38.2 | 0.4 | 1.0/0.3 | 3/2 |
| cyclohexane | 25.0 | 22.8/22.6 | 0.2 | 0.4/0.1 | 1/1 |
| decane | 23.8 | 19.6/19.6 | 0 | 0/0 | 1/1 |
| hexane | 18.4 | 9.4/9.4 | 0 | 0/0 | 1/1 |

[a] at 20°C.

The coating is also transparent (Figure 4a) and shows excellent thermal stability after rinsing. At room temperature, the wetting behavior did not change after more than one year, and in a 100°C oven, the water CA changed only slightly after 1000 hours of heating (Figure 4b); the thickness decreased by 0.6 nm during this period. Omniphobic surfaces based on

In summary, we have described a simple procedure that takes seconds to minutes (“instant”) to prepare surfaces that are omniphobic. This procedure is based on sulfuric acid catalyzed hydrolysis and step-growth graft polymerization of dimethyldimethoxysilane. This results in a smooth, slippery, covalently attached liquid (SOCAL) layer. This method requires one solution and a simple one-step procedure. This is significantly simpler

and faster than other reported methods and renders surfaces with excellent durability and omniphobic behavior that depends on surface tension in the predicted manner. The SOCAL coating shows contact angle hysteresis below 1° to liquids with a broad range of surface tensions.

Acknowledgements

We thank Gelest, Henkel, the NSF-supported Center for Hierarchical Manufacturing (CMMI-1025020), and the Materials Research Science and Engineering Center (DMR-0820506) at the University of Massachusetts for support.

Keywords: contact angle hysteresis · omniphobic surfaces · silanes · sliding angle · surface chemistry

How to cite: *Angew. Chem. Int. Ed.* **2016**, 55, 244–248
Angew. Chem. **2016**, 128, 252–256

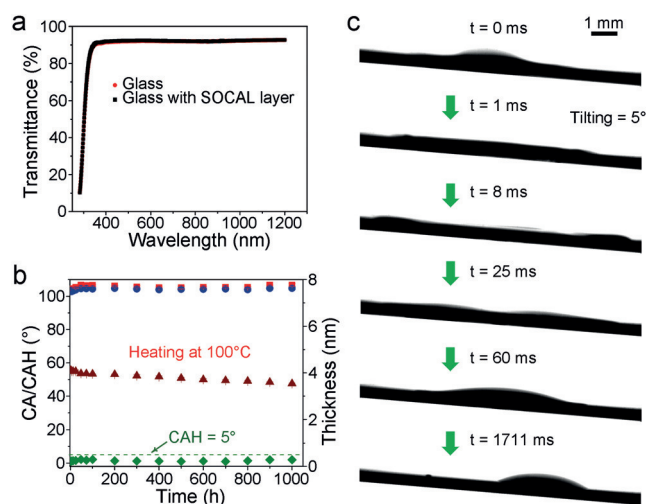


Figure 4. a) UV/Vis spectra of an untreated glass slide (●) and a slide with the SOCAL coating (■). b) Variation of the water θ_A (■), θ_R (●), and CAH ($\Delta\theta$, ◆) on a SOCAL coating and the corresponding ellipsometric thickness values (▲) as a function of aging time at 100°C. The coating was rinsed before heating. c) Time-sequence images for a 4 μL toluene drop impacting, spreading, retracting, and sliding on a SOCAL coating with an impact velocity of approximately 2.0 m s^{-1} .

topography fail at sufficient depth in liquid or when impinging drops penetrate the topographic features. The SOCAL PDMS surface reported here is smooth and stable and thus impenetrable. We used high-speed photography (Figure 4c) to monitor the impact of a 4 μL toluene drop (ca. 1.7 mm in diameter) with a velocity of 2.0 m s^{-1} on this surface. Within 1 ms of impact, the drop explosively wets the surface and spreads to a large area (ca. 9.0 mm in diameter) within about 8 ms, with a significant percentage of its volume flowing to the edge. The liquid then retracts inwards, reshapes to a sessile drop, and slides down the surface. Unlike for a reported superamphiphobic coating treated similarly,^[9a] no measurable change in omniphobicity occurred as a result of this impact.

- [1] a) W. Barthlott, C. Neinhuis, *Planta* **1997**, 202, 1; b) M. Liu, Y. Zheng, J. Zhai, L. Jiang, *Acc. Chem. Res.* **2009**, 42, 368; c) J. Zhou, D. A. Khodakov, A. V. Ellis, N. H. Voelcker, *Electrophoresis* **2012**, 33, 89; d) L. Wen, Y. Tian, L. Jiang, *Angew. Chem. Int. Ed.* **2015**, 54, 3387; *Angew. Chem.* **2015**, 127, 3448.
- [2] a) D. Quéré, *Annu. Rev. Mater. Res.* **2008**, 38, 71; b) A. R. Parker, C. R. Lawrence, *Nature* **2001**, 414, 33; c) W. Chen, A. Y. Fadeev, M. C. Hsieh, D. Oner, J. Youngblood, T. J. McCarthy, *Langmuir* **1999**, 15, 3395; d) J. Bico, C. Marzolin, D. Quéré, *Europhys. Lett.* **1999**, 47, 220; e) G. M. Whitesides, P. E. Laibinis, *Langmuir* **1990**, 6, 87.
- [3] R. J. Plunkett, US Patent US2230654, **1941**.
- [4] E. G. Rochow, US Patent US2258218, **1941**.
- [5] T. Sun, L. Feng, X. Gao, L. Jiang, *Acc. Chem. Res.* **2005**, 38, 644.
- [6] C. G. L. Furnidge, *J. Colloid Sci.* **1962**, 17, 309.
- [7] a) A. Lafuma, D. Quéré, *Nat. Mater.* **2003**, 2, 457; b) T. Onda, S. Shibuichi, N. Satoh, K. Tsujii, *Langmuir* **1996**, 12, 2125; c) Y. Tian, B. Su, L. Jiang, *Adv. Mater.* **2014**, 26, 6872.
- [8] L. Gao, T. J. McCarthy, *Langmuir* **2006**, 22, 2966.
- [9] a) X. Deng, L. Mammen, H. J. Butt, D. Vollmer, *Science* **2012**, 335, 67; b) A. Tuteja, W. Choi, M. Ma, J. M. Mabry, S. A. Mazzella, G. C. Rutledge, G. H. McKinley, R. E. Cohen, *Science* **2007**, 318, 1618; c) A. Tuteja, W. Choi, J. M. Mabry, G. H. McKinley, R. E. Cohen, *Proc. Natl. Acad. Sci. USA* **2008**, 105, 18200.
- [10] a) T. S. Wong, S. H. Kang, S. K. Y. Tang, E. J. Smythe, B. D. Hatton, A. Grinthal, J. Aizenberg, *Nature* **2011**, 477, 443; b) H. Liu, P. Zhang, M. Liu, S. Wang, L. Jiang, *Adv. Mater.* **2013**, 25, 4477; c) A. Grinthal, J. Aizenberg, *Chem. Mater.* **2014**, 26, 698.

- [11] a) D. F. Cheng, C. Urata, M. Yagihashi, A. Hozumi, *Angew. Chem. Int. Ed.* **2012**, *51*, 2956; *Angew. Chem.* **2012**, *124*, 3010;
b) J. W. Krumpfer, T. J. McCarthy, *Langmuir* **2011**, *27*, 11514.
- [12] Y. Sugahara, S. Okada, K. Kuroda, C. Kato, *J. Non-Cryst. Solids* **1992**, *139*, 25.
- [13] W. Patnode, D. F. Wilcock, *J. Am. Chem. Soc.* **1946**, *68*, 358.
- [14] J. Zhang, S. Seeger, *Angew. Chem. Int. Ed.* **2011**, *50*, 6652;
Angew. Chem. **2011**, *123*, 6782.

Received: October 7, 2015

Published online: November 16, 2015